17th World Conference on Earthquake Engineering, 17WCEE

Sendai, Japan - September 13th to 18th 2020

Experimental Study on Residual Seismic Capacity of RC Squat Walls

H. Alwashali[(1)], J. Sun [(2)], A.G. Aljuhmani[(3)], A.V. Shegay[(4)], M. Maeda[(5)], Y. Ogata[(6)], N. Aizawa[(7)]

[(1)] *Assistant professor, Graduate School of Engineering, Tohoku University, hamood@rcl.archi.tohoku.ac.jp*
[(2)] *Beijing Nuclear Star Engineering Design Co.Ltd., sjybeijingzhsd@126.com*
[(3)] *Graduate student, Graduate School of Engineering, Tohoku University, aljehmani@rcl.archi.tohoku.ac.jp*
[(4)] *Post-doctor researcher, Graduate School of Engineering, Tohoku University, ashegay@rcl.archi.tohoku.ac.jp*
[(5)] *Professor, Graduate School of Engineering, Tohoku University, maeda@archi.tohoku.ac.jp*
[(6)] *Deputy general Manager, Civil & Arch. Eng. Dept., Tohoku Electric Power Co.,Inc. ogata.yoshihiro.kv@tohoku-epco.co.jp*
[(7)] *Specialty leader, Civil & Arch. Eng. Dept., Tohoku Electric Power Co.,Inc. aizawa.naoyuki.nk@tohoku-epco.co.jp*

Abstract

Improved understanding of ground motion demands of earthquakes and advancement in seismic design has allowed engineers to build structures that will sustain limited damage after an earthquake. This has reduced the number of collapsed structures, but also increased the number of lightly to moderately damaged structures that need to be assessed, in order to repair or demolish. The 22 February 2011 Christchurch Earthquake and 2011 Great East Japan Earthquake are recent examples of this, where thousands of buildings needed to be assessed for their post-earthquake capacity. Structural engineers face a dilemma in assessing residual capacity of damaged buildings, especially for buildings with lightly to moderately damaged elements that might not need repair but require to be assessed for their performance in aftershocks and future major earthquakes.

In this regard, the buildings of Unit 2 of the Onagawa Nuclear Power Plant (NPP) experienced strong shaking levels during Great East Japan Earthquake, on March 11, 2011. The buildings of the Onagawa NPP performed well and remained within elastic range, but hairline cracks were observed in reinforced concrete (RC) shear walls. The influence of these cracks on the safety are thought not to be of a great concern due to the high safety factors in design of RC walls of the power plant buildings. However, the degradation of seismic performance due to degradation of stiffness, deformation capacity, strength and, energy dissipation needs to be clearly evaluated. There are no previous experimental studies that have clearly investigated the influence of prior damage on the seismic performance of RC squat shear walls and this was the main motivation of this study.

The main purpose of this paper is to investigate the influence of pre-damage levels on the ultimate state performance characteristics of walls, such as stiffness, shear strength, deformation and energy dissipation capacity, by conducting quasi-static cyclic loading tests of reinforced concrete shear walls. This study presents experimental results of 3 series of RC wall tests with each series having four 1\4 scale RC shear walls. The investigated parameters were: ratio of longitudinal wall reinforcement, shape of the wall boundary element and four levels of initial damage. The specimens were designed to fail in shear to represent the shear walls in nuclear power plant buildings. The seismic capacity was investigated based on the influence of the prior damage on stiffness degradation, ultimate strength, deformation capacity, and energy dissipation. The results showed that no significant deterioration was observed in ultimate strength and maximum deformation capacity due to previous damage. RC walls with flange boundary elements had greater stiffness degradation due to prior damage than rectangular walls.

Keywords: residual seismic capacity; squat RC walls; earthquake damage, nuclear power plant,

1. Introduction

Improved understanding of earthquake demands and advancement in seismic design in recent decades has allowed us to build structures with a small risk of collapse, even when subjected to large magnitude earthquakes. Although there has been a reduced the number of collapsed structures in major recent earthquakes, the number of lightly to moderately damaged structures requiring detailed assessment (to decide on repair or demolition) has increased. Recent examples include 2011 M_w 6.2 Christchurch Earthquake and 2011 M_w 9.0 Great East Japan Earthquake, where thousands of buildings needed to be reassessed for their post-earthquake capacity [1,2]. Structural engineers face a dilemma in assessing residual capacity of damaged buildings, especially for buildings with lightly to moderately damaged elements that need to be judged for their performance in aftershocks and future major earthquake.

In this regard, a guideline has been developed in Japan in 1991 for Post-Earthquake Damage Evaluation and Rehabilitation, with further revision in 2001 and 2015 [3]. Following the M_w 9.0 2011 Great East Japan Earthquake, concern was raised on the performance of squat shear walls in the Onagawa Nuclear Power Plant (NPP) buildings of Unit 2. Shear walls appeared to perform well overall and are estimated to have remained within elastic range; however, residual hairline cracks were observed in the walls after the event. The influence of these cracks on the structural safety are suspected to not be of a great concern due to the high safety factors adopted in the design of RC walls of the reactor design according to Nuclear Standards Committee [4].

Several experiments have been previously conducted to investigate the influence of loading cycles and displacement history on the seismic performance RC columns [5-7], as well for RC beams [8]. However, there are no previous experimental studies that have investigated the influences of prior damage on the future seismic performance of RC squat shear walls and thus the effect of damage on the wall stiffness degradation, deformation capacity, strength and energy dissipation is uncertain and needs to be clearly evaluated.

The purpose of this paper is to fill this gap in knowledge through experimental investigation of the influence of several pre-damage levels on the ultimate state performances of squat RC walls. The amount of pre-damage was selected by already defined damage levels in the Japanese Post Seismic Evaluation Standard [3]. As well as the damage level, other wall parameter that are considered in this study include the shape of the wall boundary element and the wall reinforcement ratio.

2. Experimental Plan

2.1 Outline of Experiment

Three series of tests were conducted (SC-13, SC-06, SF-13); each one comprised of four identical reinforced concrete shear walls. The walls were constructed with dimensions representing ¼ scale of the original shear walls of Onagawa NPP. Each of the four specimens within each series were pre-damaged to four different damage levels (by preloading of the specimens) as defined in the Japanese Standard (JBDPA 2015) (Damage Level I to Damage Level IV). The parameters varied between each series were the transverse reinforcement ratio in the shear wall, and the shape of the wall boundary elements. The longitudinal reinforcement and transverse reinforcement were applied equally for each specimen and would be referred as reinforcement ratio in this study. SC-13 represents walls with a wall reinforcement ratio of 1.3% and with columns for boundary elements (S represent shear wall, C indicates that columns are boundary elements of the wall and the number 13 represent lateral reinforcement ratio of 1.3%). Series SC-06 are shear walls with wall reinforcement ratio of 0.6% and columns as boundary elements. Series SF-13 shear walls had the same amount of reinforcement as SC-13 series, but with flanges used for boundary elements. In other words, SC-13 series and SC-06 series have the same column boundary elements but different wall reinforcement ratio, whereas in SF-13 series flange walls were used as boundary elements.

Specimens named as (0) in each series represents the undamaged wall which was tested without pre-loading to obtain full response characteristics of the original shear wall and served as the control specimens

to which damaged walls were compared. After the pre-loading phase, main loading was conducted. The description and judgment of damage levels will be described in later section of this study. Note that specimens SC-13-DII, SC-06-DII and SF-13-DI were reused as specimen SC-13-DIV, SC-06- DIV and SF-13-DIV, respectively. This is because the damage of these specimens was deemed limited and the deterioration of the capacity by pre-loading was regarded as negligible.

2.2 Test Wall Design

The specifications of the walls of all the test series are indicated in Table 1. Consistent with the walls at the Onagawa NPP all walls were designed to be shear critical. The ultimate shear strength shown in Table 1 was calculated using Eq. (1) as outlined in the AIJ standard [9-10] based on the truss and arch theory.

$$V_u = t_w l_{wb} P_s \sigma_{sy} \cot\phi + \tan\theta(1-\beta) t_w l_{wa} \nu \sigma_B / 2 \quad (1)$$

$$\beta = \{(1+\cot^2\phi) P_s \sigma_{sy}\} / \nu\sigma_B, \qquad \tan\theta = \sqrt{(h_w / l_{wa})^2 + 1} - h_w / l_{wa}$$

Where, t_w: wall thickness (mm), l_{wa}, l_{wb}: equivalent wall length (mm), P_s: shear reinforcement ratio of the wall, ν: effective compression strength coefficient, σ_{sy}: yield strength of the shear reinforcement of the wall (MPa), σ_B: compressive strength of concrete, (MPa), ϕ: angle of concrete compression strut of truss mechanism, h_w: wall height, (mm).

Dimensions and reinforcement arrangement for the three experimental series is shown in Fig. 1, Table 1 and Table 2, for all test series. Test series SC-13 and SC-06 have columns at both sides of the wall while SF-13 series walls have two flanges at both ends of the wall. The walls were cast with a foundation (concrete stub) to allow fixity to the laboratory strong floor and a concrete stub at the top through which load was applied. All the test walls have a wall panel height of 1000 mm and a thickness of 120 mm.

2.3 Loading Plan

The loading setup is shown in Fig. 2. Vertical loads were applied to the wall and columns by two vertical hydraulic jacks to maintain a constant axial stress of 0.5 MPa (total of 125 kN applied by the two vertical jacks). Cyclic horizontal load was applied simultaneously using two hydraulic jacks fixed at the mid-height of the wall as shown in Fig. 2. Thus, the inflection point was located at the at the mid-height of the wall and the resulting shear span ratio was 0.31. As illustrated in Fig. 3, the loading protocol for all series (except for walls D0) comprised of two phases: (i) application of the pre-loading until the wall reached the target damage level and (ii) reverse cyclic loading until failure.

The loading cycles for walls D0 (control specimens) in all the series consisted of two cycles at each story drift shown in Table 3, until failure. The damage observed in walls D0 at each drift angle is used as a reference, which is then used to decide the maximum drift angle that should be used in the pre-loading phase of subsequent walls in the series. The maximum drift angles in pre-loading correspond to four target damage levels: slight (damage level I), minor (damage level II), moderate (damage level III) and severe (damage level IV). The classification of damage level and details for pre-loading protocols for other specimens are discussed in the next section. As shown in Figure 3, in the pre-loading stages the walls were subjected to five cycles of loading at the target drift level, after which the wall was unloaded by gradual cyclic loading. The gradual unloading cycles were implemented to simulate a realistic ‘shake-down’ period that occurs in earthquakes. Following this unloading, the main-loading was conducted.

Table1 – Summary of test wall characteristics

	Name of specimen		SC-13 Series	SC-06 Series	SF-13 Series
	Damage class		0~IV (None～Severe)	0~IV (None～Severe)	0~IV (None～Severe)
Shear wall	Height(mm)		1000		
	Length (mm)		1800		
	Thickness (mm)		120		
	Arrangement of reinforcement		D6@40(SD295) Double	D6@80(SD295) Double	D6@40(SD295) Double
	Reinforcement ratio (%)		1.32	0.66	1.32
	Shear span to depth ratio		0.31		
Boundary confining conditions	Column	Section b×D (mm)	200×200		
		Main reinforcement	12-D16(SD345)		
		Hoop reinforcement	2-D10(SD345)@60		
	Flange wall	Height (mm)			1000
		Length (mm)			600
		Thickness (mm)			120
		Arrangement of reinforcement			D6@40(SD295) Double
		Reinforcement ratio (%)			1.32
Calculated Strength (kN) usingAIJ (1999)			Based on tested materials properties		
Shear cracking strength (kN)			571	325	429
Ultimate shear strength (kN)			1697	1343	1504
Flexural cracking strength (kN)			356	323	535
Ultimate flexural strength (kN)			4453	3852	2810

Table-2 Material properties

Name of specimen	Concrete strength Fc (N/mm^2)	reinforcement	Yield strength (N/mm^2)	Ultimate tensile (N/mm^2)
SC-13-D0	40.2	D6(SD295)	348	518
		D10(SD345)	350	572
		D16(SD345)	352	518
SC-06-D0	32.1	D6(SD295)	388	541
		D10(SD345)	364	584
		D16(SD345)	397	570
SF-13-D0	30	D6(SD295)	367	530

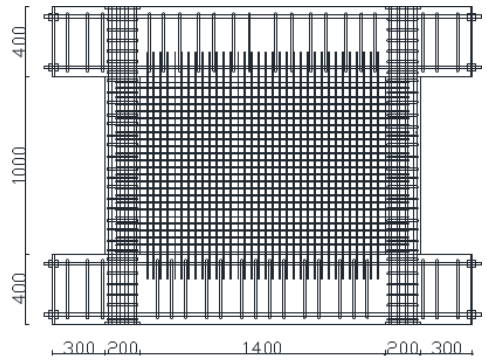

Column: Main reinforcement 12-D16(SD345)
Hoop reinforcement 2-D10(SD345) @60
Shear wall: D6@40(SD295) Double

a) Series SC-13

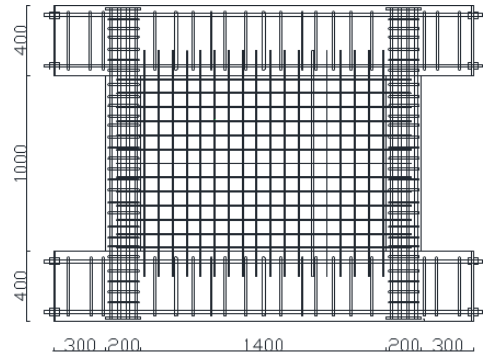

Column: Main reinforcement 12-D16(SD345)
Hoop reinforcement 2-D10(SD345) @60
Shear wall: D6@80 (SD295) Double

b) Series SC-06

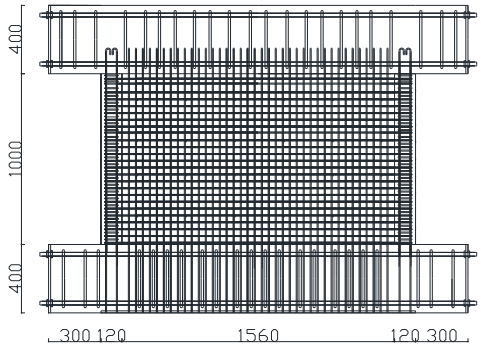

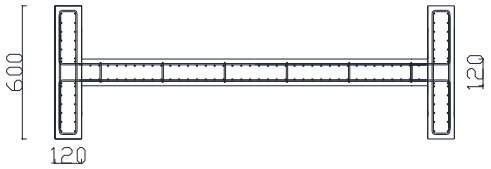

Flange wall: Arrangement of reinforcement
D6@40(SD295) Double

Shear wall: D6@40(SD295) Double

c) Series SF-13

Fig. 1 Dimension and reinforcing details of specimens (all units in mm).

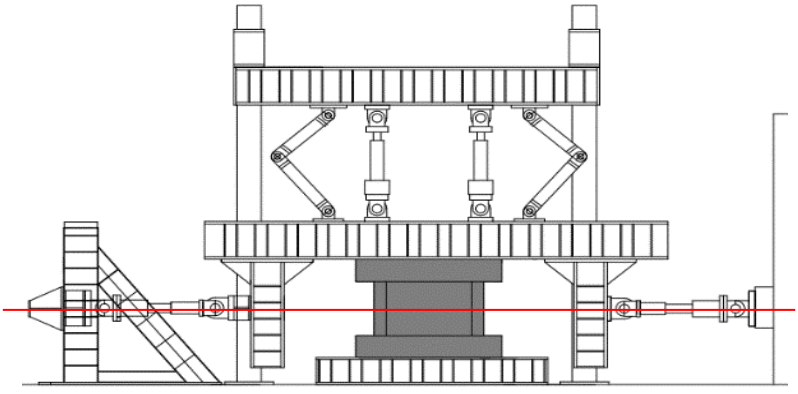

Fig. 2 – Loading setup

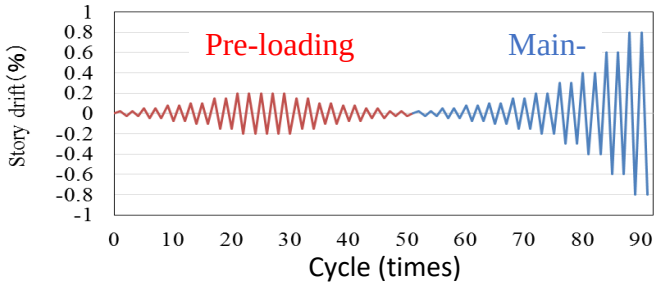

Fig. 3 Example loading history.

Table 3 –Loading schedule of control walls, -D0 (identical for all 3 test series).

Loading type*	Test Wall	Story Drift R(/1000rad.) and Number of Each Cycle *(no pre-load is applied to specimens D0)											
		±0.25	±0.5	±0.75	±1	±1.5	±2	±2.5	±3	±4	±6	±7	8
Main loading	SC-13-D0 SC-06-D0 SF-13-D0	2	2	2	2	2	2	2	2	2	2	2	2

3. Test Results: -D0 series

3.1 Shear force-displacement relationship and failure behavior of control walls

Shear force-story drift angle relationship of walls D0 are shown in Figure 4. Cracks pattern and final damage states are shown in Fig. 5.

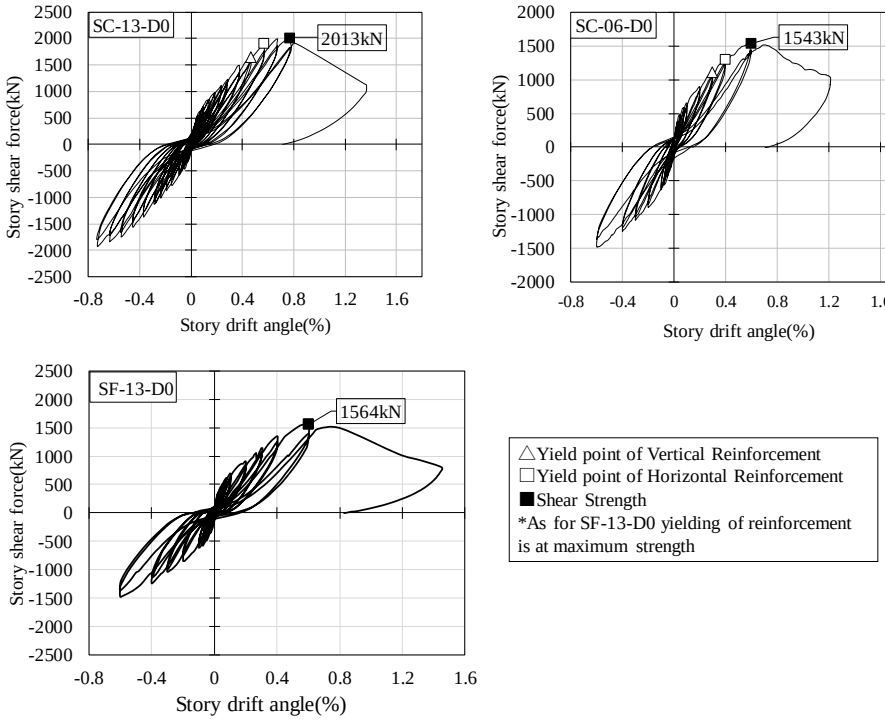

Fig. 4 Shear force-story drift relationship of -D0 walls of all series.

Cracks pattern and final damage states are shown in Fig. 5. The recording of cracks is conducted on one half of the wall face (left), assuming a symmetrical damage pattern due to symmetrical stress distribution.

Initial cracks in all walls were observed at the corners of the wall panel at story drift of 0.025%. At the cycle of story drift 0.2%, cracks developed in the entire wall panel. As for specimen SC13-D0 and SF-06-D0, with relatively high reinforcement ratio (*Ps*=1.3%), the crack spacing was found to be similar to that of the transverse reinforcement spacing. The vertical reinforcement and horizontal reinforcement yielded at story drift of 0.3%~0.4% for specimen SC-06-D0, reinforcement ratio of *Ps*=0.66%, which is slightly earlier than of SF-13-D0, which yielded at 0.5%~0.6% drift. The maximum shear force was reached at a story drift of 0.8% for specimen SC-13-D0, and at a story drift of 0.6% for specimen SC-06-D0 and SF-13-D0. At this point, concrete spalling was also observed. Just after reaching maximum strength, there was a rapid drop of shear strength resulting in severe crushing of concrete in the web of the walls.

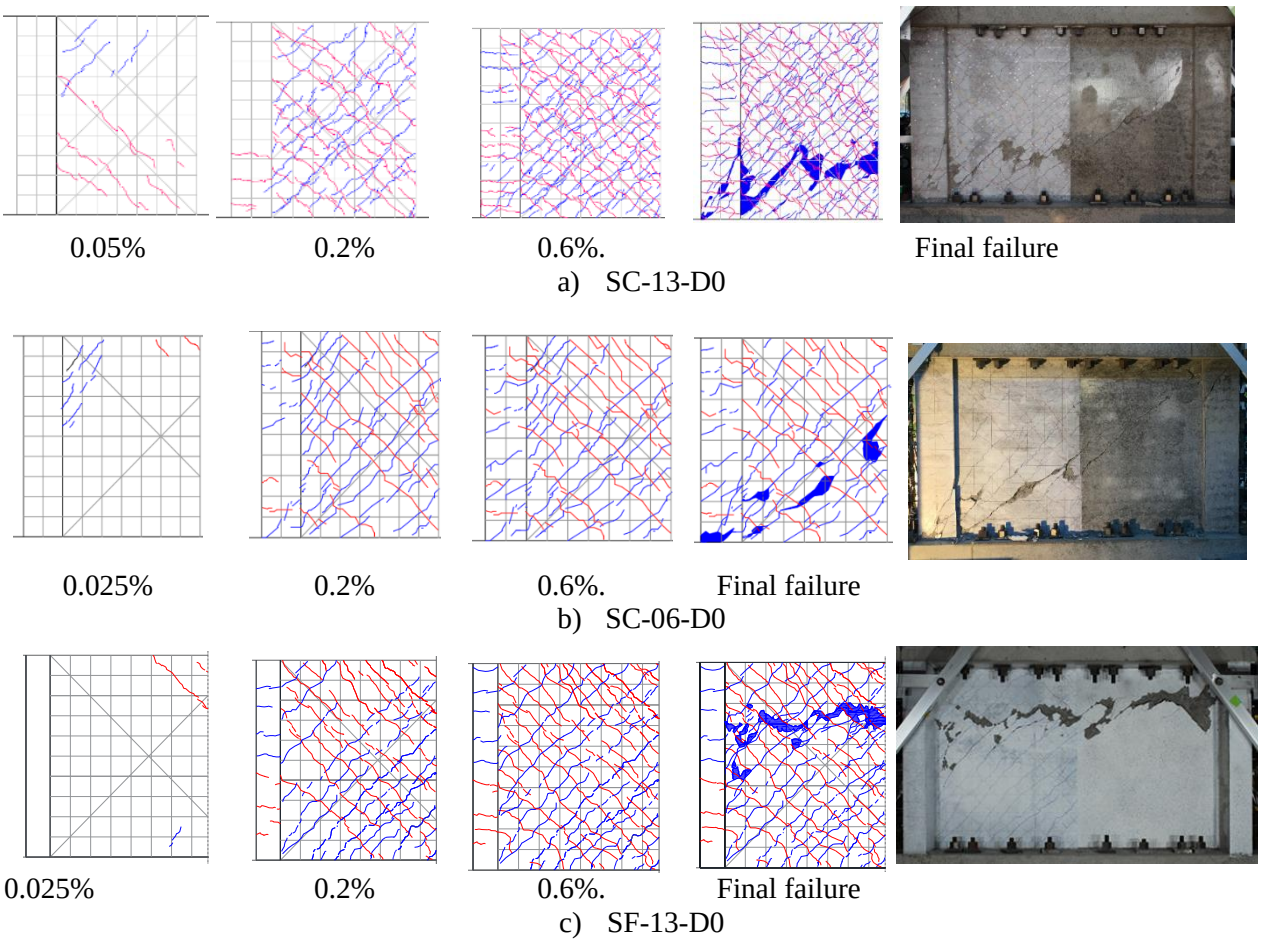

Figure 5 Cracking patterns of SC-13-D0, SC-06-D0, SF-13-D0

3.2 Classification of Damage Class in Control Walls D0 in all series

In the JBDAP standard [3], damage of structural elements is classified into five classes described in Table 3 and illustrated in Fig. 6, based on damage characteristics such as the maximum residual crack width, spalling of concrete, and buckling or fracture of steel reinforcement. In this paper, damage classes in the shear walls (SC-13-D0, SC-06-D0 and SF-13-D0) are judged based on the JBDAP standard [3]. In addition, the load-deflection curve, stiffness degradation ratio and yielding states of the reinforcement as well as the crack width are considered to determine those damage classes and their corresponding story drift.

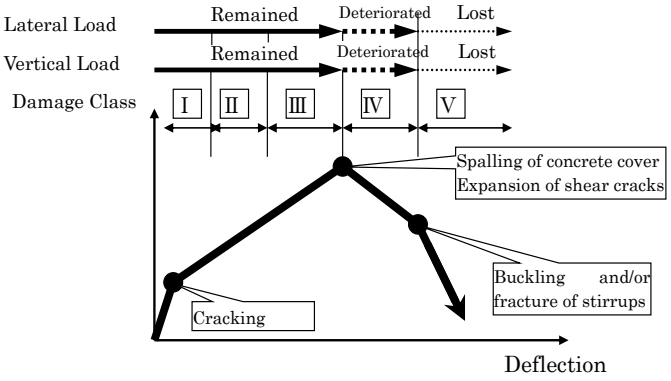

Fig. 6: Idealized lateral force-displacement curve with damage classes based on [3]

Table 3 – Damage classes of structural elements from [3]

Damage class	Damage situation
I	Concrete cracks are found. Crack width is smaller than 0.2 mm.
II	Cracks of 0.2 - 1 mm wide are found.
III	Wide cracks of 1 - 2 mm wide are found. Some spalling of concrete is observed.
IV	Many wide cracks are found. Crack width is larger than 2 mm. Reinforcing bars are exposed due to spalling of the cover concrete.
V	Buckling of reinforcement, crushing of concrete and vertical deformation of columns and/or shear walls are found. Side-sway, subsidence of upper floors, and/or fracture of reinforcing bars observed.

Using these criteria and by comparison with the observed damage in specimens D0, it was determined for all test series, that a drift of less than 0.1% corresponds to damage class I; 0.1%~0.3% drift corresponds to damage class II; 0.3%~0.5% drift corresponds to damage class III, and the drift of 0.5% drift to ultimate shear strength corresponds to damage class IV. The division between these damage classes are shown on the wall backbone response in Fig. 7. Based on this definition, the pre-loadings protocols for specimens S-DI~DIV were carried out, as shown in Table 4.

Table 4– Loading schedule of damaged specimens: DI~DIV (All of Series)

	Pre-Loading													
	Story Drift R(/1000rad.) and Number of Each Cycle (Time)													
Wall	±0.25	±0.5	±0.75	±1	±2	±3	±4	±6	±4	±3	±2	±1	±0.5	±0.25
DI	2	5	5										2	2
DII	2	2	2	2	5							2	2	2
DIII	2	2	2	2	2	2	5			2	2	2	2	2
DIV	2	2	2	2	2	2	2	5	2	2	2	2	2	2

	Main Loading										
	Story Drift R(/1000rad.) and Number of Each Cycle (Time)										
Wall	±0.25	±0.5	±0.75	±1	±1.5	±2	±2.5	±3	±4	±6	Final
DI~DIV	2	2	2	2	2	2	2	2	2	2	2

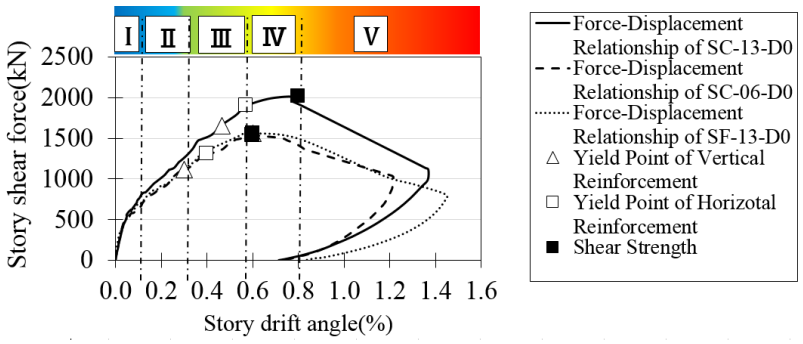

Fig. 7 Relationship between the assigned damage class and lateral force-displacement backbone.

4. Experimental results of the experiment: DI ~ DIV-of all series

4.1 Shear force-story drift angle relationship of damaged specimen

Shear force-story drift angle relationship in the positive loading of all the pre-damaged walls (DI ~ DIV) for all the test series is shown in Fig. 8. For all test series, all the pre-damaged walls showed similar damage progression to the walls D0 (with no pre-damage). As shown in Fig.8, the stiffness degradation and relatively smaller hysteresis loops are observed until the point of preloading, after that the shear walls behaved similar to the undamaged walls, this observation is discussed later section of this study. As previously mentioned, specimens SC-13-DII, SC-06-DII and SF-13-DI were not loaded to failure as they were reused as tests SC-13-DIV, SC-06- DIV and SF-13-DIV, respectively. This was done because the level of pre-damage in these tests was judged to be in the elastic region and damage was insignificant.

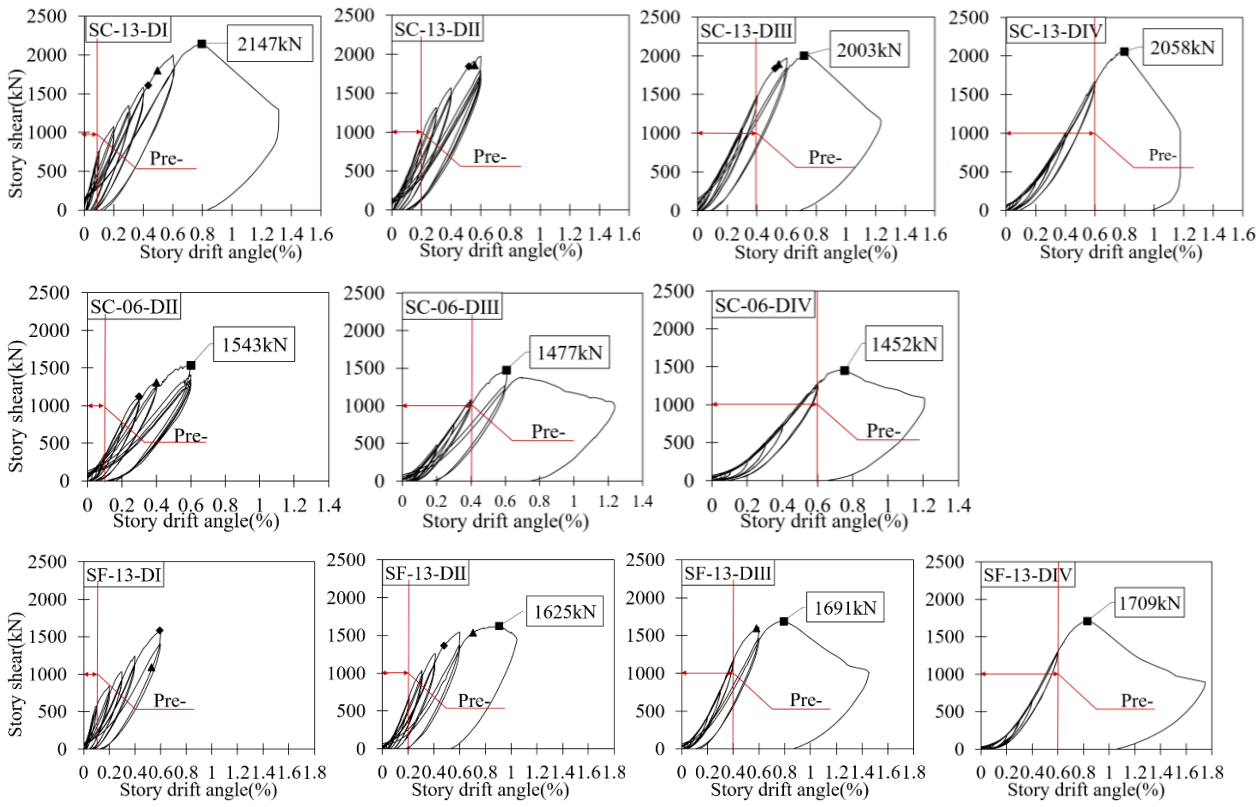

Fig. 8: Shear force-story drift angle relationship of damaged specimens.

4.2 Comparison of stiffness degradation.

The relationship between story drift and secant stiffness degradation is illustrated in Figure 9. The stiffness of all of the pre-damaged specimens in each series are compared to the initial stiffness of the same specimen at the pre-loading phase. The initial stiffness is calculated based on the initial loading to the 0.025% drift. While for the rest of the cycles, stiffness is calculated based on the slope of the line connecting the positive and negative peak point at each cycle. It is noticed that even for damage class I that experienced small deformation and limited damage during the pre-damage phase, the initial stiffness decreased by approximately a factor of two compared to the D0 wall tests. It can also be noticed that the secant stiffness decreases as the pre-damage level increases. For all pre-damaged walls, beyond the experienced deformation in the pre-loading phase, almost no secant stiffness difference is observed compared to the undamaged specimen D0 in each series. From Figure 9, it can be seen that the walls in series SC-06 with a lower reinforcement ratio (0.6%) experience more rapid and more severe stiffness degradation compared to the walls in series SC-13 (reinforcement ratio of 1.3%).

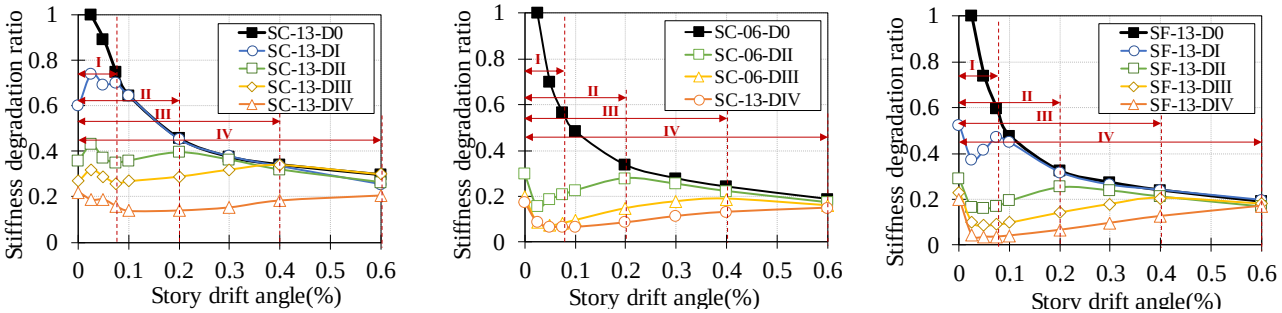

(a) (b) (c)

Fig. 9 Secant stiffness as a ratio of the uncracked wall stiffness for (a) Series SC-13; (b) Series SC-06 and (c) SF-13

4.3 Comparison of shear strength and deformation capacity

Envelopes of the shear force – story drift for all the specimens in each series are demonstrated in Figure 10. For each test series, at every point of the pre-damaged wall preceding the target story drift which represent the pre-loading limit, the capacity of the wall is less than that for the undamaged specimen D0. This is attributed to the degradation of stiffness as discussed in the previous section and shown in Figure 9. For test series SC-13 and SF-13 (walls with relatively high reinforcement ratio), beyond the target story drift for each pre-damage state, there is no meaningful difference in the load demand when compared to the undamaged D0 tests, as shown in Figure 11. In the SC-06 series, the walls with pre-damage levels III-IV showed a slight reduction (approximately 10%) from the maximum shear force achieved in the D0 walls, but this observation is not conclusive since the number of specimens is limited. The results showed that no significant deterioration was observed in ultimate strength and maximum deformation capacity due to previous damage. Though similar results have been found in experimental studies on residual capacity of flexural-governed component [8], this is the first study to demonstrate no significant effect of prior damage on the strength capacity for shear-governed components.

In this study, deformation capacity is defined as a 20% drop of load capacity from a previous observed maximum. As shown in in Fig. 10 and similar to observations for residual strength capacity, the deformation capacity does degrade as a result of any level of pre-damage induced in this study. In series SC-13 and SF-13, the deformation capacity increase for large levels of pre-damage.

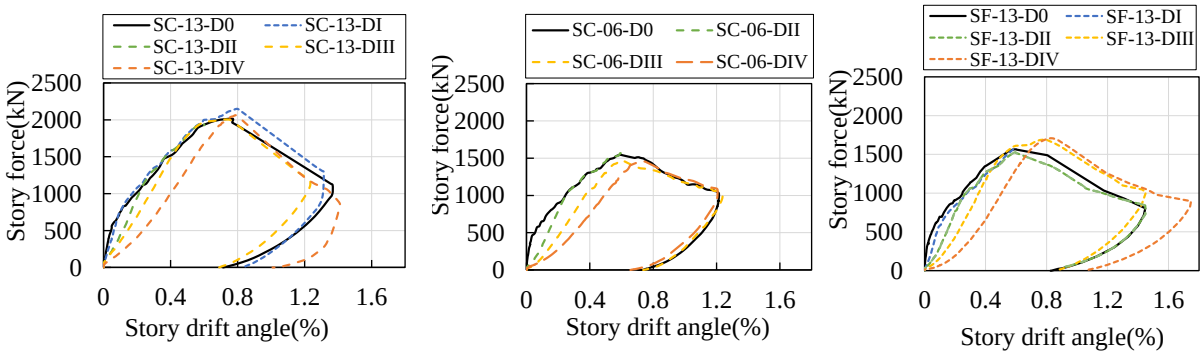

Fig. 10 envelope of shear force – story drift curves for different damage level

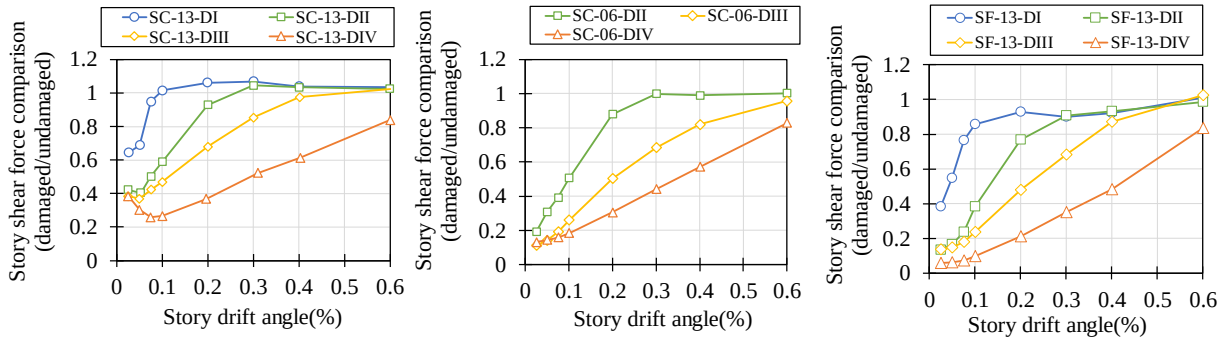

Fig. 11 Lateral force at each drift of the damaged specimens as a ratio of the undamaged specimen results.

4.4 Comparison of energy dissipation capacity

Energy absorption of one cycle is determined as the area inside the hysteresis loop of that cycle. The degradation of energy absorption capacity could be judged by the ratio of loop area of the pre-damaged specimens to the loop area of specimen without pre-damage (D0). The changes of loop area ratio are shown in Fig. 12. In SC-13 series and SC-06 series, at the small story drift angles of even less than 0.1%(<XXX%), the energy absorbing capacity of pre-damaged specimens was degraded by 40~80% depending to the damage levels. However, when the story drift of the wall extends beyond the pre-damage drift, the energy dissipation capacity of the pre-damaged specimens in SC-13 series is equal to that of the D0 specimens (i.e., loop area ratio is nearly equal to 1.0). Specimens in series SF-13, with boundary element as flange wall, showed higher degradation in loop area than other series, this could be due to confinement by boundary element is smaller for flange walls than boundary element as column.

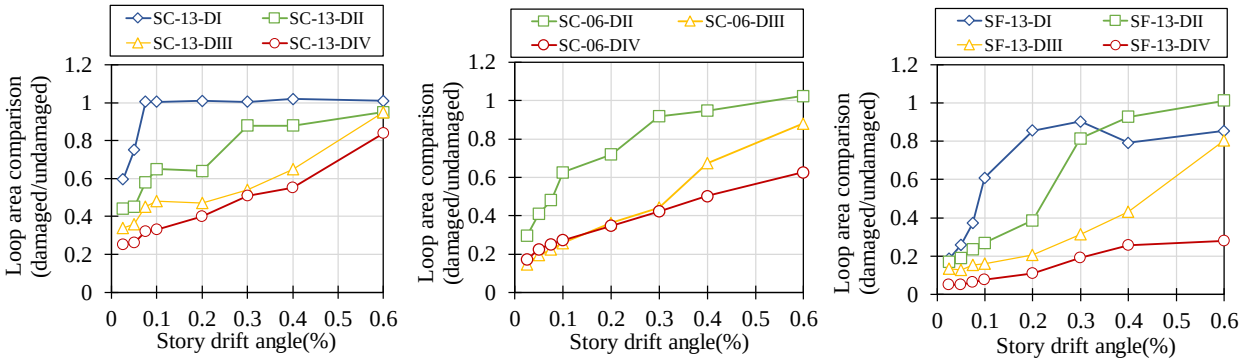

Fig. 12 Ratio of loop area at each cycle of the pre-damaged specimens to the control specimen D0

6. CONCLUSION

Following minor cracking damage to squat RC walls in the Onagawa Nuclear Power Plant, concerns were raised regarding the performance of these walls in future earthquake events. To assess the residual capacity of squat RC walls, ¼ scale RC walls were tested using quasi-static cyclic loading. The tests were divided into three series (four walls per series) with the parameters investigated between series being two levels of wall reinforcement ratio and boundary element geometry and the parameters investigated within each series being four levels of initial damage. The specimens were designed to exhibit a shear-failure mechanism to represent a real concrete shear walls in nuclear power plant buildings. The objective of tests is to clarify the influence of prior damage on the seismic capacity of shear walls based on influence of prior damage. The following key conclusions are drawn from this study:

1) The results showed rapid and severe stiffness degradation in squat walls subjected to initial levels of damage. Reaching damage level I according to [3], resulted in secant stiffness reduction of 30% for walls with rectangular boundary elements, and up to 60% for walls with flanged boundary elements.
2) The results showed that no significant deterioration was observed in wall ultimate strength capacity and maximum deformation capacity due to any level of previous damage.
3) Specimens pre-damaged of SF 13 series (flange boundaries) have greater stiffness degradation and a smaller energy dissipation capacity relative to walls with column boundary elements. The specimens with a lower reinforcing ratios showed a slight degradation of strength of less than 10 % when subjected to prior damage level IV (Severe damage), but those results are inconclusive due to the limited number of specimens tested.
4) The relationship between prior damage level and observed degradation of stiffness is obtained which is useful in remodelling of damaged RC walls using modified backbone curve.

7. REFERENCES

[1] K.J. Elwood, F. Marquis and J. H. Kim "Post-Earthquake Assessment and Repairability of RC Buildings: Lessons from Canterbury and Emerging Challenges" Proceedings of the Tenth Pacific Conference on Earthquake Engineering Building an Earthquake-Resilient Pacific 6-8 November 2015, Sydney, Australia

[2] Maeda, M., Alwashali, H., Takahashi K., and Suzuki K., "Damage of RC Building Structures due to 2011 East Japan Earthquake" Proceedings of 2012 Structures Congress. ASCE. pp.1023-1034, 2012.3

[3] Japan Building Disaster Prevention Association, Standard for Post-earthquake Damage Level Classification of Buildings, 2016.3 (in Japanese)

[4] Nuclear Standards Committee. "Technical Code for Seismic Design of Nuclear Power Plants", JEAC4601-2008

[5] Iwasaki, T.; Kawashima, K.; Hasegawa, K.; Koyama, T.; and Yoshida, T.,"Effect of Number of Loading Cycles and Loading Velocity of Reinforced Concrete Bridge Piers," Structural Eng. /Earthquake Eng. Vol. 5. No, 1, 183s-191s. April 1988 Japan Society of Civil Engineers (Proc, of JSCE No. 392/1-9)

[6] Pujol S, Sozen MA, Ramirez JA. (2006). Displacement history effects on drift capacity of reinforced concrete columns. ACI Struct J. 2006;103(2):253.

[7] A. Nojavan, A.E. Schultz, and S-H. Chao "effect of lateral loading protocols on seismic performance of RC columns" Proceedings of the 11th National Conference in Earthquake Engineering, Earthquake Engineering Research Institute, Los Angeles, CA. 2018

[8] Marder, K. J., Motter, C. J., Elwood, K. J., and Clifton, G. C. (2018). "Effects of variation in loading protocol on the strength and deformation capacity of ductile reinforced concrete beams." Earthquake Engineering & Structural Dynamics, 47(11), 2195‐2213.

[9] Architectural Institute of Japan (AIJ). (1999). "Design Guidelines for Earthquake Resistant Reinforced Concrete Building Based Inelastic Displacement Concept" (in Japanese)

[10] Architectural Institute of Japan (AIJ). (2010). "AIJ Standard for Structural Calculation of Reinforced Concrete Structures" (in Japanese)

